nature chemistry

ARTICLES

PUBLISHED ONLINE: 1 APRIL 2012 | DOI: 10.1038/NCHEM.1314

Multiphase design of autonomic self-healing thermoplastic elastomers

Yulin Chen†, Aaron M. Kushner†, Gregory A. Williams and Zhibin Guan*

The development of polymers that can spontaneously repair themselves after mechanical damage would significantly improve the safety, lifetime, energy efficiency and environmental impact of man-made materials. Most approaches to self-healing materials require the input of external energy, healing agents, solvent or plasticizer. Despite intense research in this area, the synthesis of a stiff material with intrinsic self-healing ability remains a key challenge. Here, we show a design of multiphase supramolecular thermoplastic elastomers that combine high modulus and toughness with spontaneous healing capability. The designed hydrogen-bonding brush polymers self-assemble into a hard–soft microphase-separated system, combining the enhanced stiffness and toughness of nanocomposites with the self-healing capability of dynamic supramolecular assemblies. In contrast to previous self-healing polymers, this new system spontaneously self-heals as a single-component solid material at ambient conditions, without the need for any external stimulus, healing agent, plasticizer or solvent.

The ability to spontaneously heal injury is a key biomaterial feature that increases the survivability and lifetime of most plants and animals. In sharp contrast, synthetic materials usually fail after damage or fracture. For decades, scientists and engineers have dreamed of developing self-healing materials to improve the safety, lifetime, energy efficiency and environmental impact of man-made materials[1,2]. Most approaches to self-healing materials require the input of external energy in the form of heat[3–5] or light[6–8]. Of the few spontaneously self-healing polymers, some need healing agents (monomers and catalysts)[9,10] and others are soft materials that require substantial solvation (gels)[11–13] or plasticization (rubber)[14,15]. Despite intense research in this field[16–18], the synthesis of a stiff material with intrinsic self-healing ability remains a key challenge[19].

For most designs, external energy is required to achieve healing. For example, thermally reversible covalent bonds[3,20,21] or non-covalent supramolecular linkages[4] have been introduced into polymers that, upon heating, can reversibly rupture and reform to provide self-healing. Recently, a metallo-supramolecular polymer was shown to be thermally mendable by converting photonic energy into localized heat[6]. In this microphase-separated system, the metal-complex healing motifs reside in the crystalline hard domain, which requires thermal energy to reversibly dissociate in order to heal. For many applications, however, autonomic healing without any external stimulus is desirable. With this in mind, an elegant dynamic supramolecular approach was developed to obtain a self-healing rubber using multivalent hydrogen bonds[15], which, although individually weak, collectively form a load-bearing network that is dynamic at room temperature[22], allowing autonomic healing of damage. Nevertheless, this system requires substantial plasticization to enhance the molecular dynamics, and the single-phase dynamic assembly of short oligomers limits this approach to low-modulus rubber applications. For most supramolecular designs there is an inherent compromise between mechanical stiffness and dynamic healing; strong interactions result in stiff but less dynamic systems, precluding autonomous healing, and weak interactions afford dynamic healing, but yield soft materials.

Herein, we report a novel multiphase design that can combine stiffness and spontaneous healing in a thermoplastic elastomeric system. The key to this new design was to program dynamic healing motifs (hydrogen bonds) in the soft phase of a hard–soft multiphase system (Fig. 1), merging the unique properties of hybrid polymers (stiffness and toughness) with those of dynamic supramolecular assemblies (autonomic healing). This is analogous to the design of thermoplastic elastomers (TPEs), which use a multiphase morphology to combine the elasticity of rubbers with stiffness previously only accessible to thermoplastics, dramatically expanding the material landscape available to engineering applications[23]. Typically, TPEs are block- or brush-copolymers that microphase separate into 'hard' glassy or crystalline domains embedded in a 'soft' rubbery matrix. The hard domains not only serve as physical crosslinks to ensure rubber elasticity, but also contribute to the high modulus and stiffness of TPEs. The covalent character of the soft segments between the hard domains, however, precludes self-healing for classical TPEs at temperatures below the glass transition (T_g) or melting temperature (T_m) of the hard phase. We reasoned that if we could replace the covalent connectivity in the soft segments with a non-covalent, supramolecular soft matrix, we might obtain self-healing TPEs (Fig. 1).

To demonstrate our concept, we developed a hydrogen-bonding brush polymer (HBP) that self-assembles into a two-phase morphology that behaves as a true TPE, that is, combining high Young's modulus and extensibility. Importantly, our system spontaneously heals as a single-component solid material under ambient conditions, without the need for any external stimulus, healing agent, plasticizer or solvent. The HBP consists of a 'hard' backbone (high T_g) and 'soft' brushes (low T_g) carrying polyvalent hydrogen-bonding sites for dynamic supramolecular assembly (Fig. 1). Previous theoretical studies predict that amphiphilic brush copolymers self-assemble into the desired spherical morphology in an appropriate polar solvent via collapse of the hydrophobic core[24,25]. For our self-healing TPE system (Fig. 1a), we chose a polystyrene backbone as the hard phase and polyacrylate amide (PA-amide) brushes as the soft phase. The pendent secondary

Department of Chemistry, 1102 Natural Sciences 2, University of California, Irvine, California 92697, USA; †These two authors contributed equally to this work. *e-mail: zguan@uci.edu

© 2012 Macmillan Publishers Limited. All rights reserved.

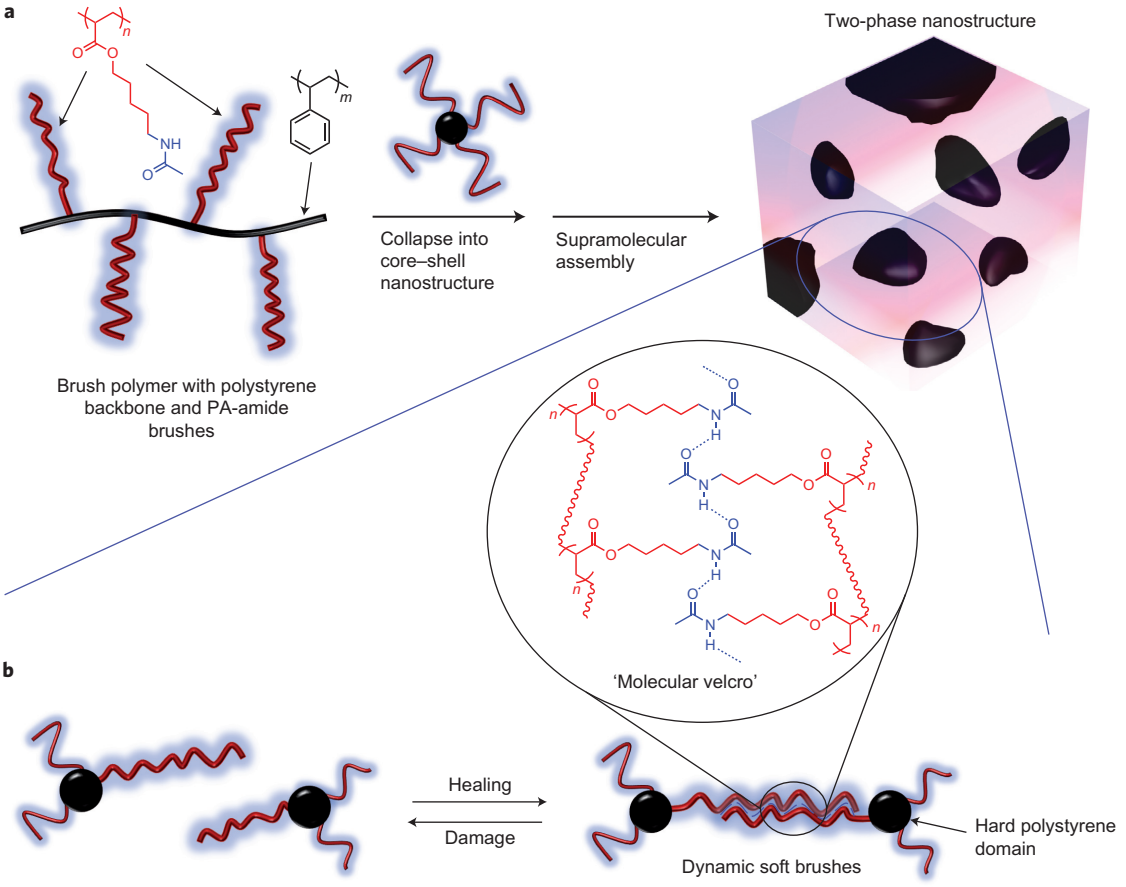


Figure 1 | Design concept for the multiphase self-healing brush polymer system. a, The hydrogen-bonding brush polymer self-assembles into a two-phase nanostructure morphology during processing. The hydrogen bonds are individually dynamic, but polyvalent clusters of covalently linked associative hydrogen-bonding interactions result in a mechanically stable connection that behaves like a permanent covalent linkage. **b**, Although mechanically robust, the supramolecular connections between soft brushes can rupture reversibly under stress, in contrast to conventional TPE systems, where rupture of the purely covalent interdomain connections is irreversible.

amide functional group is simple to synthesize and capable of forming dynamic networks, having both hydrogen bond donor and acceptor functionality. Previous studies have shown that a thermodynamically weak but pervasive network of dynamic hydrogen bonds nonetheless affords mechanical robustness on the relevant timescales. Processed from a polar solvent, the brush polymer should collapse into a core–shell nanostructure with a hard polystyrene core and a soft PA-amide shell. Hydrogen-bonding-directed supramolecular assembly of the PA-amide brushes should lead to the formation of a dynamic microphase-separated nanostructure that can be reversibly broken and reformed, affording spontaneous self-healing behaviour (Fig. 1b).

Results and discussion

Materials synthesis. Synthesis of the HBPs is described in Fig. 2. An acrylate amide monomer **1** was designed for polymerization of the self-healing soft brushes. We selected a secondary amide as a simple reversible hydrogen-bonding motif. A five-carbon spacer was introduced into **1** to lower the glass transition temperature (T_g) of the PA-amide brush and enhance the flexibility of the hydrogen-bonding terminal amide. The desired monomer **1** was obtained after an efficient two-step synthesis from inexpensive starting materials. The polystyrene backbone was synthesized by free-radical polymerization. Multiple radical initiation sites were introduced for subsequent soft-brush growth using atom transfer radical polymerization (ATRP)[26]. The well-defined synthesis allows for precise control of molecular parameters such as backbone and brush length, density of the brushes and hydrogen-bonding motifs, providing tunability of the mechanical properties of the polymer. For our initial demonstration, the brush length and density were varied to afford three **HBP**s **1**–**3**, with varying polystyrene weight fraction (Table 1). Two control polymers, an HBP with hydrogen-bond-blocked tertiary amide monomer **2** (**Control-2**) and a simple linear polymer of **1** (**Control-1**), were also synthesized to enable comparative studies.

Material characterizations. The molecular weight and size (radius of gyration, R_g) of the polymers were determined by multi-angle laser light scattering (MALLS) following size-exclusion chromatography with methanol as the eluent (Table 1). The number-average molecular weights (M_n) agree well with the values estimated from the number of ATRP initiation sites and monomer conversion measured by ^{1}H NMR spectroscopy, indicating the high efficiency and 'living' character of the ATRP brush polymerization. The hydrodynamic radius (R_h) of the polymers was measured by dynamic light scattering (DLS). The ratio R_g/R_h for **HBP**s **1**–**3** is ~0.7 (Table 1), indicating a globular morphology[27] as a result of collapse of the hydrophobic polystyrene backbone in polar methanol. In contrast, the ratio R_g/R_h is ~2 for the linear homopolymer of **1** (**Control-1**), confirming its expected random coil conformation in a good solvent[27].

The light-scattering data confirm that individual macromolecules adopt the desired globular morphology in a polar solution. As the bulk polymer samples were prepared by slow solvent

© 2012 Macmillan Publishers Limited. All rights reserved.

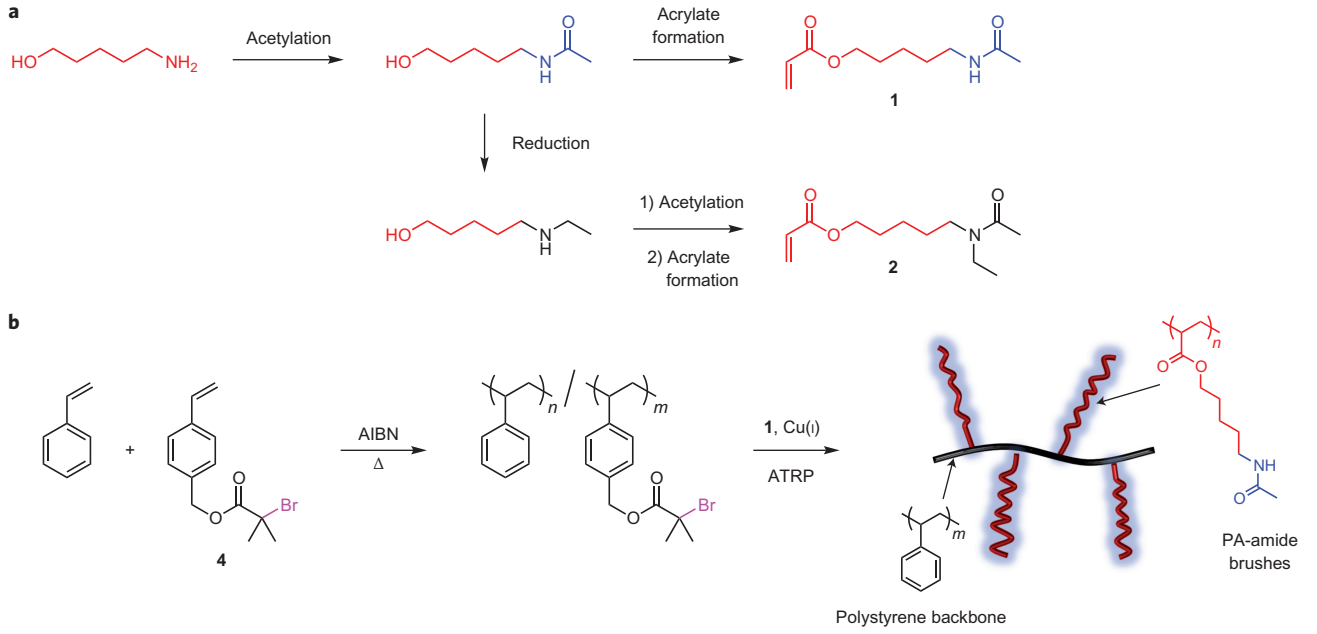


Figure 2 | Synthesis of monomers and brush polymers. a, Synthesis of hydrogen-bonding monomer **1** and the hydrogen-bond-blocked control monomer **2**. **b**, Synthesis of HBPs. Styrene was first copolymerized with an ATRP co-monomer **4** via free-radical polymerization, followed by ATRP polymerization of monomer **1** to form the brushes. **Control-2** was prepared in the same manner by using monomer **2** in the brush formation.

evaporation of polymer solutions in methanol, we assume that the morphology will be preserved in the solid state. Indeed, transmission electron microscopy (TEM) imaging of **HBP-3** reveals a two-phase morphology, with nanospheres (polystyrene) dispersed in a continuous matrix (PA-amide) (Fig. 3d). The radius of the polystyrene nanospheres is <20 nm, with the larger domains presumably composed of multiple brush polymers. Small-angle X-ray scattering (SAXS) of the bulk material (Fig. 3c) shows a broad, intense scattering peak indicating the presence of well-defined spherical form-factor domains with inter-domain spacings ranging from 5–40 nm for brush polymer **HBP-3** (the linear **Control-1** showed no peak). The apparent broad peak in the **HBP-3** spectrum around 14 nm indicates a spherical domain form factor, with a nanodomain spacing comparable to the macromolecular size as determined by MALLS (Table 1).

Mechanical studies. **HBP**s **1**–**3** are amorphous non-tacky solids with a T_g for the soft matrix below room temperature (ranging from 2 °C to 5 °C), and are suited for thermoplastic elastomer applications at room temperature. The key mechanical properties of **HBP**s **1**–**3** and the two control polymers are summarized in Table 2. Static stress–strain curves of **HBP**s **1**–**3** follow the shape of those of classical TPEs (Fig. 3a), with a high initial stiffness followed by large elastic deformation (310–1,570%). The Young's moduli of **HBP**s **1**–**3** are about two orders of magnitude higher than the previously reported self-healing thermoreversible rubber system[15], which has mechanical properties comparable to a classical rubber (Fig. 3a, inset). When the samples were left in open air to fully equilibrate with moisture, the moduli and strength of the HBPs dropped by ~20%. The elastomeric properties of HBPs were further confirmed by creep recovery (Fig. 3b) and stress–relaxation experiments (Supplementary Fig. S1). At 25 °C, a stress of 4×10^4 Pa applied to **HBP-3** for 800 min resulted in a strain of ~35%, which increased at a rate of 0.02% per hour. After releasing the applied stress, the sample completely recovered its dimensions with negligible residual strain (<1%). Applying a medium stress (1.2×10^5 Pa) for the same amount of time led to a strain of ~110%, which increased at a rate of 0.04% per hour. Release of the stress left a residual strain of less than 5%. Applying a high stress (2×10^5 Pa) under the same conditions resulted in a strain of ~170% with an incremental increase of 0.07% per hour. Release of the stress left a residual strain of ~17%. Tensile stress–relaxation experiments (Supplementary Fig. S1) further confirmed the elastomeric properties of **HBP**s **1**–**3**. Both static stress–strain and time-dependent mechanical tests (creep recovery and stress–relaxation) demonstrate that, although the hydrogen bonds are individually weak and dynamic, collectively they can form a robust network that can sustain significant load for an extended period[22]. Although a purely dynamic elastomer completely devoid of

Table 1 | Summary of molecular characterizations of HBPs 1-3 and control samples.

Sample	Polystyrene backbone repeat units (Br/chain)	PA-amide brush repeat units	$M_n \times 10^{-3}$ g mol^{-1} (^{1}H NMR)*	$M_n \times 10^{-3}$ g mol^{-1} (MALLS)†	PDI†	R_h (nm)‡	R_g (nm)†	R_g/R_h
HBP-1	114 (11)	186	455	435	1.3	25.5	18	0.7
HBP-2	114 (11)	84	203	197	1.5	20.5	14	0.7
HBP-3	100 (5)	194	197	193	1.3	23.5	14	0.6
Control-1	-	193	39	40	1.25	7.5	15.7	2.1
Control-2	114 (11)	220	584	558	1.1	20	22	1.1

*Estimated from monomer conversion as measured by ^{1}H NMR spectroscopy. †Measured by size-exclusion chromatography (SEC) with a multi-angle laser light scattering detector (MALLS). ‡Measured by dynamic light scattering (DLS). PDI is the polydispersity index of a polymer, which is calculated by M_w/M_n.

© 2012 Macmillan Publishers Limited. All rights reserved.

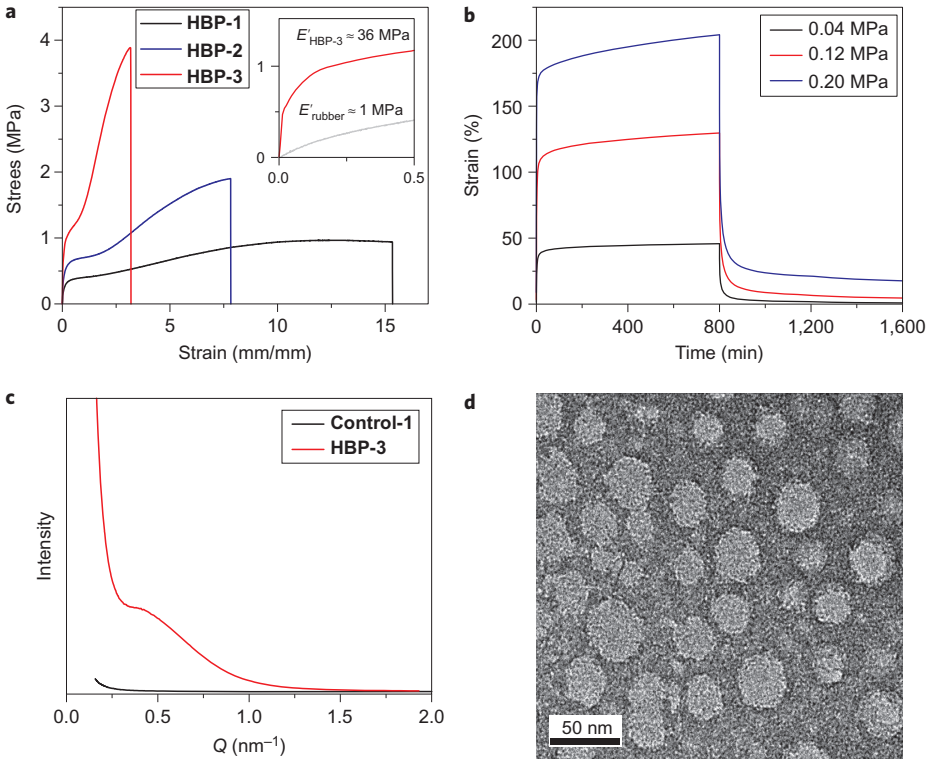


Figure 3 | Characterization of the basic bulk mechanical properties and multi-phase morphology of HBPs. a, Static tensile tests of **HBPs 1–3** illustrates the TPE-like stress–strain behaviour, as well as demonstrating tunability of the mechanical properties via rational molecular design. Inset: the tensile behaviour of **HBP-3** is compared with natural rubber. **b**, Creep-recovery behaviour at different stress levels closely follows that of covalently linked elastomers. **c**, SAXS data support the microphase-separated morphology, while the linear **Control-1** shows no scattering peak. *Q*, scattering factor. **d**, TEM imaging provides clear evidence of a microphase-separated structure with a spherical polystyrene core dispersed in a soft PA-amide matrix, which was selectively stained with uranyl acetate.

Table 2 | Summary of mechanical and self-healing properties.

	Mechanical properties						Self-healing (% recovery of extensibility)	
Sample	Young's modulus* (MPa)	Yield strength† (MPa)	Strain-at-break* (%)	Strength-at-break* (MPa)	G′‡ (MPa)	G″‡ (MPa)	1 h	24 h
HBP-1	9.8±1.1	0.26±0.02	1570±40	0.9±0.05	2.2	4.5	42±2	79±2
HBP-2	17.3±0.3	0.48±0.02	780±15	1.92±0.18	4.6	12	51±3	90±4
HBP-3	35.7±3.4	0.89±0.04	310±6	3.77±0.32	5.5	16.3	40±1	75±2
Control-1	–§	–	–	–	0.24	0.39	–	–
Control-2	–	–	–	–	0.05	0.07	–	–

*Strain rate=100 mm min^{-1}, 25 °C. †Taken as strength at 10% strain. ‡25 °C, 1 Hz oscillation, 1% strain. §The controls are mechanically weak and could not be cast into films for tensile testing.

covalent crosslinks may not be able to maintain static high loads indefinitely[15], many elastomer applications involve primarily cyclic, rather than static, load conditions. Our materials should be suitable for such engineering applications.

Previous studies have shown that well-defined strong hydrogen-bonding modules[28,29] or pervasive weaker hydrogen-bonding motifs[14,15] are effective for forming supramolecular polymers with elastic properties. In our HBPs, polyvalent hydrogen-bonding interactions connect the soft PA-amide brushes between hard polystyrene domains, resulting in TPE properties. Chain entanglement between the PA-amide brushes should not play a major role here. First, based on data for poly(*n*-butyl acrylate)[30], the entanglement chain length for PA-amide should be ~190 repeat units. For **HBPs 1–3**, the PA-amide brush lengths are around or below this value. Second, simply blocking the hydrogen-bonding amides of a brush polymer (**Control-2**) completely destroys the elasticity and results in a dramatically weaker material (Table 2). In agreement with our multiphase design concept, the polystyrene hard phase contributes critically to the initial stiffness and thermoplastic elastomer behaviour. Without the polystyrene core, the homopolymer of **1**, **Control-1**, is a very weak elastomer (Table 2). Importantly, the synthetic versatility of our system allows for systematic tuning of the structure and the corresponding mechanical properties. For example, by varying the styrene weight fraction from 3 to 7%, we are able to tune the Young's modulus *E* by a factor of three without compromising the material's self-healing ability (Fig. 3a, Table 2).

Self-healing studies. In our multiphase supramolecular design, we envisioned that the reversible hydrogen bonding in the soft matrix should afford self-healing properties. Indeed, **HBPs 1–3** exhibit spontaneous self-healing behaviour at room temperature without introducing any plasticizer, solvent, healing agents or external

© 2012 Macmillan Publishers Limited. All rights reserved.

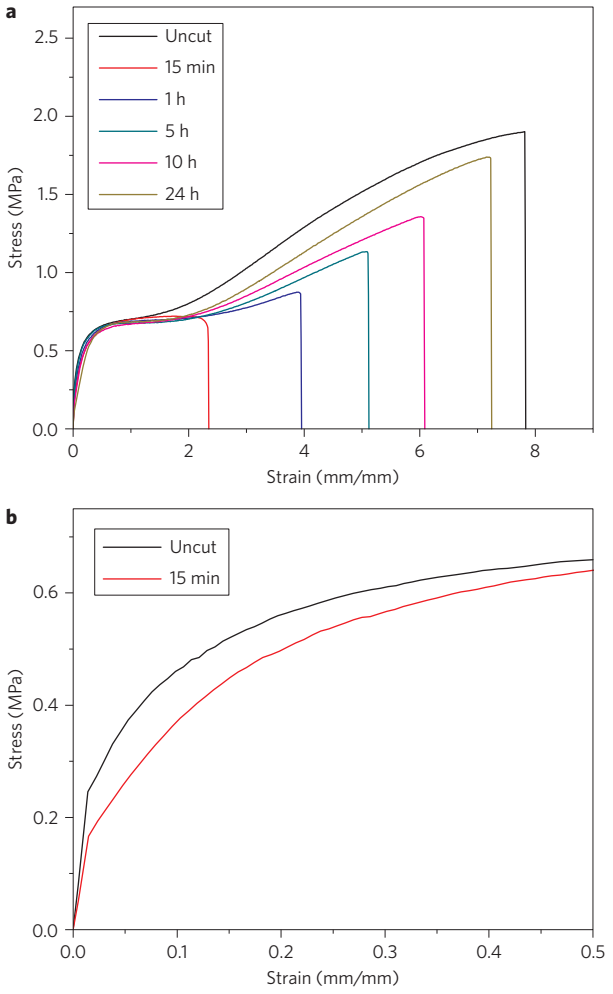


Figure 4 | Self-healing tests for HBP-2 at room temperature. a, The sample was cut into completely separate pieces using a razor blade and the cut faces were gently brought together and allowed to heal at 25 °C for various times. **b**, Initial tensile behaviour of a cut sample healed only for 15 min is compared with the stress–strain curve of the pristine sample. The initial modulus, yield strength, and stress at 50% strain for the healed sample are very close to the values of the pristine sample.

stimuli. After cutting a sample into two completely separate pieces with a razor blade and gently bringing the cut pieces back into contact, the two faces spontaneously self-heal over time under ambient conditions without any treatment (Supplementary video). For all healing times, stress–strain curves show characteristic TPE behaviour and follow closely the shapes of the original uncut samples. Longer healing times lead to better healing, with optimal healing of up to 92% recovery of extensibility relative to a pristine sample (Fig. 4a). Notably, the initial modulus, yield strength and stress at 50% strain, well above the operational window for many compressive rubber applications such as vibrational isolation[30], recover almost quantitatively after only 15 min of healing time (Fig. 4b). **HBP-1** is the most extensible and **HBP-3** is the stiffest and strongest of the HBPs, but **HBP-2** seems to have a good balance of hard and soft phases and has the most impressive self-healing property (Supplementary Fig. S9).

We further investigated the effect of separation time on the self-healing ability of the HBPs. Similar to the observation of a previous hydrogen-bonding self-healing rubber system[15], longer waiting times between cutting and facial re-contact result in reduced mechanical property recovery (Supplementary Fig. S10). This can be attributed to the dangling hydrogen bonds exposed on the freshly cut surface, over time, becoming increasingly likely to find co-facial interaction partners, thus reducing their availability as molecular stitches when the surfaces are brought back into contact. In most applications, however, this time-dependent healing behaviour might be irrelevant, because the system should spontaneously start to heal immediately following microcrack formation.

The essential role of the dynamic hydrogen bonds contributing to HBPs' unique TPE behaviour and self-healing properties is best illustrated in the following control experiment. By simply blocking the hydrogen-bonding capability, **Control-2** polymer completely loses its TPE characteristics and behaves as a viscous fluid unsuitable for static stress–strain testing. The storage modulus for **Control-2** as measured by rheology is almost two orders of magnitude lower than that of **HBP-1** (Table 2), which has an otherwise identical molecular structure as the control polymer. These studies confirm that the polyvalent dynamic hydrogen bonding is responsible for the mechanical properties of the material, and is crucial to the unique self-healing behaviour.

Conclusions

This work demonstrates a new multiphase design strategy for autonomic healing materials that can combine important mechanical properties such as high modulus and high elasticity and toughness. In contrast to previous self-healing polymers[3,10,15], our HBP system achieves spontaneous self-healing as a single-component solid material without any external stimuli, healing agents, plasticizer or solvent. Furthermore, the well-defined design and synthesis offers versatility in tuning the structures and properties. A number of molecular parameters (such as the backbone, brush and supramolecular healing motif) can be systematically tuned both for optimizing the polymer properties and gaining a fundamental understanding of this system. Finally, our multiphase design concept for self-healing materials should be generally applicable to a wide range of other multiphase supramolecular systems, including graft and block copolymers with various morphologies, functional nanoassemblies and organic–inorganic nanocomposites. We are currently pursuing many facets of these studies in our laboratory.

Methods

Details of materials synthesis and structural characterizations can be found in the Supplementary Information.

Morphology characterization. TEM was performed on a FEI/Philips CM-20 conventional TEM operated at an accelerating voltage of 200 kV. The polyacrylate amide phase was stained by floating the TEM grid on a 0.5 wt% aqueous solution of uranyl acetate for 1 min, followed by removal of excess solvent by placing the sample on filter paper. SAXS studies were carried out at the Materials Research Laboratory of the University of California, Santa Barbara. Exact details of the homebuilt SAXS set-up can be found at http://www.mrl.ucsb.edu/mrl/centralfacilities/xray/instruments/saxs.html.

Mechanical testing. The mechanical properties of the copolymers were measured using an Instron 3365 machine in standard stress/strain experiments. Samples were prepared by hot-pressing the resin into Teflon moulds. The specimens were extended at 100 mm min^{-1} at room temperature. Each measurement was repeated at least three times. Young's modulus was determined from the initial slope of the stress–strain curves. Creep recovery and stress–relaxation experiments were performed using a TA Instruments DMA Q800 with attached cryo accessory. The films were pulled at a certain stress for 800 min, and then the stress was released and the films were recovered for another 800 min at 25 °C. In stress–relaxation tests, the samples were pulled at a rate of 10 or 100 mm min^{-1} to reach 100% strain (set at this strain for relaxation for 800 min; Supplementary Fig. S1). Rheology data were collected on an AR G2 rheometer from TA Instruments (20 mm parallel steel plate). Time sweep experiments were performed to obtain the moduli of the materials at 1 Hz and 1% strain at 25 °C.

Sample damaging and healing tests. For self-healing tests, a sample was cut into two completely separate pieces. The cut faces were gently pressed together for 1 min and then left to heal in a desiccator at room temperature for various times. The self-healed samples were then subjected to stress–strain tests at room temperature at a pulling rate of 100 mm min^{-1} (Supplementary Fig. S9).

© 2012 Macmillan Publishers Limited. All rights reserved.

Received 17 November 2011; accepted 23 February 2012; published online 1 April 2012

References

1. Shinya, N. *Frontiers of Self-Healing Materials and Applications* (CMC Publishing Co., 2010).
2. Ghosh, S. K. *Self-Healing Materials: Fundamental, Design Strategies, and Applications.* (Wiley-VCH, 2009).
3. Chen, X. *et al.* A thermally re-mendable cross-linked polymeric material. *Science* **295,** 1698–1702 (2002).
4. Burattini, S. *et al.* A healable supramolecular polymer blend based on aromatic π–π stacking and hydrogen-bonding interactions. *J. Am. Chem. Soc.* **132,** 12051–12058 (2010).
5. Klukovich, H. M., Kean, Z. S., Iacono, S. T. & Craig, S. L. Mechanically induced scission and subsequent thermal remending of perfluorocyclobutane polymers. *J. Am. Chem. Soc.* **133,** 17882–17888 (2011).
6. Burnworth, M. *et al.* Optically healable supramolecular polymers. *Nature* **472,** 334–337 (2011).
7. Amamoto, Y., Kamada, J., Otsuka, H., Takahara, A. & Matyjaszewski, K. Repeatable photoinduced self-healing of covalently cross-linked polymers through reshuffling of trithiocarbonate units. *Angew. Chem. Int. Ed.* **50,** 1660–1663 (2011).
8. Ghosh, B. & Urban, M. W. Self-repairing oxetane-substituted chitosan polyurethane networks. *Science* **323,** 1458–1460 (2009).
9. Toohey, K. S., Sottos, N. R., Lewis, J. A., Moore, J. S. & White, S. R. Self-healing materials with microvascular networks. *Nature Mater.* **6,** 581–585 (2007).
10. White, S. R. *et al.* Autonomic healing of polymer composites. *Nature* **409,** 794–797 (2001).
11. Wang, Q. *et al.* High-water-content mouldable hydrogels by mixing clay and a dendritic molecular binder. *Nature* **463,** 339–343 (2010).
12. South, A. B. & Lyon, L. A. Autonomic self-healing of hydrogel thin films. *Angew. Chem. Int. Ed.* **49,** 767–771 (2009).
13. Imato, K. *et al.* Self-healing of chemical gels cross-linked by diarylbibenzofuranone-based trigger-free dynamic covalent bonds at room temperature. *Angew. Chem. Int. Ed.* **50,** 1–5 (2011).
14. Montarnal, D., Tournilhac, F., Hidalgo, M., Couturier, J.-L. & Leibler, L. Versatile one-pot synthesis of supramolecular plastics and self-healing rubbers. *J. Am. Chem. Soc.* **131,** 7966–7967 (2009).
15. Cordier, P., Tournilhac, F., Soulie-Ziakovic, C. & Leibler, L. Self-healing and thermoreversible rubber from supramolecular assembly. *Nature* **451,** 977–980 (2008).
16. Syrett, J. A., Becer, C. R. & Haddleton, D. M. Self-healing and self-mendable polymers. *Polym. Chem.* **1,** 978–987 (2010).
17. Murphy, E. B. & Wudl, F. The world of smart healable materials. *Prog. Polym. Sci.* **35,** 223–251 (2010).
18. Burattini, S., Greenland, B. W., Chappell, D., Colquhoun, H. M. & Hayes, W. Healable polymeric materials: a tutorial review. *Chem. Soc. Rev.* **39,** 1973–1985 (2010).
19. Sottos, N. R. & Moore, J. S. Materials chemistry: spot-on healing. *Nature* **472,** 299–300 (2011).
20. Bergman, S. D. & Wudl, F. Mendable polymers. *J. Mater. Chem.* **18,** 41–62 (2008).
21. Chen, X., Wudl, F., Mal, A. K., Shen, H. & Nutt, S. R. New thermally remendable highly cross-linked polymeric materials. *Macromolecules* **36,** 1802–1807 (2003).
22. Ciferri, A. Bond scrambling and network elasticity. *Chem. Eur. J.* **15,** 6920–6925 (2009).
23. Holden, G., Kricheldorf, H. R. & Quirk, R. P. (eds) *Thermoplastic Elastomers* 3rd edn (Hanser, 2004).
24. Borisov, O. V. & Zhulina, E. B. Amphiphilic graft copolymer in a selective solvent: intramolecular structures and conformational transitions. *Macromolecules* **38,** 2506–2514 (2005).
25. KoSovan, P. *et al.* Amphiphilic graft copolymers in selective solvents: molecular dynamics simulations and scaling theory. *Macromolecules* **42,** 6748–6760 (2009).
26. Patten, T. E., Xia, J., Abernathy, T. & Matyjaszewski, K. Polymers with very low polydispersities from atom transfer radical polymerization. *Science* **272,** 866–868 (1996).
27. Burchard, W. Static and dynamic light scattering from branched polymers and biopolymers, in *Light Scattering from Polymers* Vol. 48, 1–124 (Springer, 1983).
28. Sijbesma, R. P. *et al.* Reversible polymers formed from self-complementary monomers using quadruple hydrogen bonding. *Science* **278,** 1601–1604 (1997).
29. Folmer, B. J. B., Sijbesma, R. P., Versteegen, R. M., van der Rijt, J. A. J. & Meijer, E. W. Supramolecular polymer materials: chain extension of telechelic polymers using a reactive hydrogen-bonding synthon. *Adv. Mater.* **12,** 874–878 (2000).
30. Zosel, A. & Ley, G. Influence of crosslinking on structure, mechanical properties, and strength of latex films. *Macromolecules* **26,** 2222–2227 (1993).

Acknowledgements

This work was partially supported by the US Department of Energy, Division of Materials Sciences (award no. DE-FG02-04ER46162), corporate gifts and the University of California, Irvine. The authors thank Youli Li at the University of California, Santa Barbara, for assistance with using SAXS at the MRL Central Facilities at UC Santa Barbara supported by the MRSEC Program of the NSF (award no. DMR05-20415).

Author contributions

Z.G., Y.C. and A.M.K. planned the experiments, Y.C., A.M.K. and G.A.W. conducted the experiments, Z.G., Y.C. and A.M.K. analysed the data, and Z.G., A.M.K., Y.C. and G.A.W. wrote the paper.

Additional information

The authors declare no competing financial interests. Supplementary information and chemical compound information accompany this paper at www.nature.com/naturechemistry. Reprints and permission information is available online at http://www.nature.com/reprints. Correspondence and requests for materials should be addressed to Z.G.

© 2012 Macmillan Publishers Limited. All rights reserved.